

A Lattice Boltzmann method for simulations of liquid-vapor thermal flows

Raoyang Zhang and Hudong Chen

Exa Corporation, 450 Bedford Street, Lexington, MA 02420

(October 23, 2018)

Abstract

We present a novel lattice Boltzmann method that has a capability of simulating thermodynamic multiphase flows. This approach is fully thermodynamically consistent at the macroscopic level. Using this new method, a liquid-vapor boiling process, including liquid-vapor formation and coalescence together with a full coupling of temperature, is simulated for the first time.

arXiv:physics/0210054v1 [physics.flu-dyn] 11 Oct 2002

I. INTRODUCTION

After years of research, the Lattice Boltzmann Methods (LBM) has become an established numerical approach in computational fluid dynamics (CFD). Many models and extensions have been formulated that cover a wide range of complex fluids and flows [1]. Furthermore, LBM has been extended to include turbulence models that have already had a direct and substantial impact on engineering applications [3,4,5,6].

Among many desirable LBM features such as simplicity, parallelizability, and robustness in dealing with complex boundary conditions, one recognized advantage is its capability of simulating fluid flows with multiple phases [10,11,1]. The core mechanism in LBM modeling of multiphase flows is its microscopic level realization of non-ideal gas equations of state. As a result, at sufficiently low temperature and proper pressure, liquid-vapor like first order phase transitions are spontaneously generated. There is no need to explicitly tracking the interfaces between immiscible phases. Furthermore, unlike static statistical physical models [12], LBM also contains the momentum conservation, so that bubbles and liquid droplets are formed along with fluid hydrodynamic processes. The success and simplicity of LBM for multiphase flows has led to various applications that include simulations of oil-water mixtures through porous media [7], Rayleigh-Taylor problems [8,11], and many more [1]. On the other hand, there is an crucial missing piece. That is, so far all the existing multiphase LBM models are limited to regimes in which the temperature dynamics is either negligible or its effect on flow is unimportant. This limitation, along with the overall unavailability in CFD, has prevented us from dealing with an important class of flows, namely multiphase flows involving strong couplings with thermodynamics. Specific examples of such type of flows range from the common water boiling processes to thermal nuclear reactor applications. Thus from both fundamental and practical point of views, extensions of the existing CFD and LBM methods to simulation of thermal multiphase flows is extremely important.

The LBM is originally evolved from lattice gas models obeying fundamental conservation laws and symmetries [2,13,14,15]. Now it has also been shown to be systematically derivable

from the continuum Boltzmann equation [16]. The most commonly known lattice Boltzmann equation (LBE) has the following form (adopting the lattice units convention in which $\Delta t = \Delta x = 1$),

$$f_i(\mathbf{x} + \hat{c}_i, t + 1) - f_i(\mathbf{x}, t) = \mathcal{C}_i, \quad (1)$$

where time t takes on only positive integer values, and the particle velocity takes on a finite set of discrete vector values (speeds), $\{\hat{c}_i; i = 0, \dots, b\}$. These speeds form links among nodes on a given lattice [2,9]. The collision term on the right hand side of eqn.(1) now often uses the so called Bhatnagar-Gross-Krook (BGK) approximation [17,9],

$$\mathcal{C}_i = -\frac{f_i - f_i^{eq}}{\tau}, \quad (2)$$

having a single relaxation time parameter, τ . Here, f_i^{eq} is the local equilibrium distribution function that has an appropriately prescribed functional dependence on the local hydrodynamic properties. The basic hydrodynamic quantities, such as fluid density ρ and velocity \mathbf{u} , are obtained through simple moment summations,

$$\begin{aligned} \rho(\mathbf{x}, t) &= \sum_i f_i(\mathbf{x}, t), \\ \rho \mathbf{u}(\mathbf{x}, t) &= \sum_i \hat{c}_i f_i(\mathbf{x}, t). \end{aligned} \quad (3)$$

In addition, one can also define a fluid temperature T from,

$$\rho \frac{D}{2} T(\mathbf{x}, t) = \sum_i \frac{1}{2} (\hat{c}_i - \mathbf{u}(\mathbf{x}, t))^2 f_i(\mathbf{x}, t), \quad (4)$$

where D is the dimension of the momentum space of the discrete lattice velocities [2]. It has been theoretically shown that the hydrodynamic behavior produced from LBE obeys the Navier-Stokes fluid dynamics at a long wave-length and low frequency limit [9]. The resulting equation of state is that of an ideal gas fluid, namely the pressure p obeys a linear relation with density and temperature,

$$p = \rho T. \quad (5)$$

The kinematic viscosity of the fluid is related to the relaxation parameter by [2,4,9]

$$\nu = (\tau - \frac{1}{2})T. \quad (6)$$

LBM has been extended to simulations of multiphase flows [1,10,11]. The key step is to introduce an additional term, $\Delta f_i(\mathbf{x}, t)$ on the right hand side of eqn.(1), to represent a body-force. This force term is self-consistently generated by the neighboring distribution functions around each lattice site, and it does not either violate the local mass conservation nor the global momentum conservation. However, the local momentum is altered by an amount,

$$\mathbf{F}(\mathbf{x}, t) = \sum_i \hat{c}_i \Delta f_i(\mathbf{x}, t). \quad (7)$$

The appearance of the body force term can be physically, in a mean-field sense, attributed to a non-local interacting potential U among the particles [19]. The existence of such an interacting potential is the essential mechanism in the non-ideal gas type of fluids. Hence with a suitable choice of U , spontaneous phase separations can be produced, and one can use it conveniently to numerically study multiphase flow phenomena. Through the years, there have been many progresses in LBM models for multiphase flows [1]. On the other hand, as pointed out at the beginning, all the existing attempts are limited to isothermal (or “a-thermal”) situations in which the dynamics of temperature in the fluid is suppressed. That is, T is either assumed a constant or, at best, a prescribed function of space (or time).

II. MULTIPHASE FLOWS WITH INCORPORATION OF THERMODYNAMICS

In this paper, we present an extension of multiphase LBM to include the full thermodynamic process.

The most natural extension in LBM for thermodynamics has been to introduce a conserved energy degree of freedom [20]. This is relatively straightforward for the ideal gas type of models in which only pointwise collisions are involved and only kinetic energy is

considered. When a sufficient number of particle speeds is used, one can theoretically show that LBM leads to the correct full set of thermohydrodynamic equations of an ideal-gas fluid [4,20,21]. Unfortunately, besides being considerably more expensive computationally than the isothermal LB models, such an approach cannot be easily generalized to multiphase thermodynamic flows. The most obvious obstacle is the difficulty in tracking the energy evolution while maintaining a total energy conservation: For a non-ideal gas system, the total energy also contains an interacting energy part that is a function of the relative positions among the particles. Without a total energy conservation, a temperature variable cannot be defined fully self-consistently at the microscopic level. In addition, it has been shown that, unlike the isothermal models, an LBE with an energy degree of freedom does not guarantee a global H -theorem [23]. As a consequence, the system can exhibit significantly less stability. Other undesirable features in this direct approach include 1) difficulty in changing Prandtl number value from unity, unless a substantial generalization to the BGK collision term is made; and 2) a rather limited temperature range (with the maximal allowable value only about twice the minimal value), unless significantly more speeds are added [4,21]. Because of these reasons, the progress in LBM for thermal multiphase flows has been rather slow.

Here we present a new LBM approach that can essentially avoid all of the above mentioned drawbacks. The fundamental idea can be briefly summarized: First of all, the fluid dynamics part (i.e., the density and momentum evolution) is represented by a modified *isothermal* LBE, while the energy evolution part is determined by an additional scalar energy transport equation [22]. The latter can be solved either via a finite difference scheme or an auxiliary LBE. Secondly, the coupling of the two parts is through a properly defined body force term in the LBE (and the compression and dissipation terms in the energy equation). As we shall realize below, although conceptually rather simple, the new model produces the correct full thermohydrodynamic equations together with a non-ideal gas equation of state.

We choose a common isothermal LBE (e.g., D3Q19, [9]) as a starting basis. As discussed earlier, an isothermal LBE model for fluid density and velocity evolution is considerably simpler compared to its energy conserving counterpart. This is certainly desirable for doing

efficient fluid flow simulations. Furthermore, the equilibrium distribution in an isothermal LB model is only a function of fluid density and velocity. The lack of temperature dynamics in the equilibrium distribution is the key for achieving a higher stability in LBE [23]. Having these in mind, it is much desirable to introduce a macroscopic mechanism to recover thermodynamics. Specifically, instead of letting temperature to influence the equilibrium distributions in an LB system, the thermodynamic effect is obtained via a temperature-dependent body-force [10]. Because of the “external” nature of the coupling, the LB system and its equilibrium property remain to be microscopically isothermal. Nonetheless, as explained below, this alternative way of coupling achieves the desired thermodynamics at the macroscopic level.

Ignoring the higher order contributions, the body-force term can be simply expressed as [18],

$$\Delta f_i(\mathbf{x}, t) = \frac{w_i}{T_0} \hat{c}_i \cdot \mathbf{F}, (\mathbf{x}, t) \quad (8)$$

where the constant weights w_i and T_0 are directly determined by the LBE model (e.g., D3Q19; in which $T_0 = 1/3$). One can easily verify that this gives rise to eqn.(7). The global momentum conservation is preserved as long as $\mathbf{F}(\mathbf{x}, t)$ is expressed as a spatial gradient of a scalar function [24],

$$\mathbf{F}(\mathbf{x}, t) = -\nabla U(\mathbf{x}, t). \quad (9)$$

It is straightforward to implement this condition in a discrete space by proper finite-difference procedures. Based on the consideration for higher order isometry in surface tension, we choose (for D3Q19) the following specific form,

$$\nabla U(\mathbf{x}, t) \approx \sum_i \frac{D}{bc_i^2} \hat{c}_i U(\mathbf{x} + \hat{c}_i, t) \quad (10)$$

With the additional body-force term, one can easily recognize that the overall effective pressure in the resulting fluid momentum equation has become,

$$p = \rho T_0 + U \quad (11)$$

where the first term is a result of the isothermal LBM. From (11), one can obtain any form of equation of state, $p = p(\rho, T)$, simply by making a corresponding choice for U ,

$$U(\mathbf{x}, t) = p(\rho(\mathbf{x}, t), T(\mathbf{x}, t)) - \rho(\mathbf{x}, t)T_0. \quad (12)$$

The above quantity is determined once the local values of $\rho(\mathbf{x}, t)$ and $T(\mathbf{x}, t)$ are provided. Obviously the resulting fluid is no longer isothermal if the temperature $T(\mathbf{x}, t)$ varies. In other words, because of the macroscopic way of coupling, the resulting fluid dynamics is no longer isothermal. In addition, with the high flexibility of choosing the equation of state, this approach can be applied to simulation of non-ideal gas fluids and multiphase flows. Indeed, we confirmed this basic feature through a set of spinodal decomposition tests based on a Van de Waals gas model (Carnahan-Starling equation of state). Similar to the other multiphase LBM, a spontaneous phase separation process is well observed at sufficiently low temperature values.

The evolution of the temperature $T(\mathbf{x}, t)$ in this new approach is obtained from solving a supplemental scalar energy transport equation,

$$\rho(\partial_t + \mathbf{u} \cdot \nabla)e = -p\nabla \cdot \mathbf{u} + \nabla \cdot \kappa \nabla T + \Psi \quad (13)$$

where $e = c_v T$ is the internal energy, and c_v is the specific heat at constant volume of the fluid. The overall pressure p is defined by the equation of state (11), and κ is the heat conductivity that can be specified flexibly. The term Ψ represents the viscous dissipation of flow and the contribution of surface tension. The energy evolution equation (13) is a standard macroscopic description for thermal fluids [19]. The computation of an isothermal LB model along with a scalar energy equation is considerably less expensive than any microscopic attempts: for it neither requires many particle speeds nor complicated tracking of the energy evolution. Moreover, the difficulties in stability and Prandtl number associated with the original thermal LBM are not issues in this approach. Solving a scalar transport equation is rather straightforward. There are many finite-difference schemes for accurately and efficiently solving the scalar transport equation. In our particular simulations, we have

used an extended Lax-Wendroff scheme [5]. The combination of eqns. (1)-(3), (8)-(10), and (12)-(13) forms the new LBM approach for modeling multiphase thermodynamic fluid flows. The thermal boundary condition can be realized via standard numerical procedures so that,

$$\kappa \hat{n} \cdot \nabla T|_w = q, \quad (14)$$

with a prescribed heat flux q , that can either be fixed or a function of local properties in order to achieve a fixed wall temperature. The unit vector \hat{n} denotes the surface normal direction.

There is one more important feature in this model worth pointing out. That is, the new approach avoids the fundamental limitation on the temperature range that has constrained the other thermal LB models. Notice the temperature only appears in the body-force term in a gradient function form. Hence, unlike that for equilibrium distribution functions, there is no absolute upper or lower bound on the temperature values except that it should not change too rapidly across a given resolution scale. Moreover, there is obviously no absolute bound on temperature in the energy equation.

Based on the above discussions, one can realize that the new LB model generates a fully macroscopically consistent description for thermodynamic flows involving generalized equations of state. Therefore, this approach offers a convenient and efficient numerical tool for studying thermal multiphase flow problems.

III. SIMULATION OF THE LIQUID-VAPOR BOILING PROCESS

In this section we present computational results of a typical multiphase thermodynamic flow simulation with the new LB approach. In particular, a liquid-vapor boiling process involving Rayleigh-Benard like convections, phase changes, together with a complex temperature dynamics is simulated successfully, albeit qualitative. Although representative of a wide range of important applications, boiling flow problems have received little success from CFD in general. Consequently, it is very important that the new approach can demonstrate such a fundamental capability.

The Rayleigh-Benard convection process has been widely used as a benchmark for many fluid computations. It is the simplest representation of a boiling phenomenon in which a complex buoyancy-driven convection process occurs at various values of the Rayleigh number [25]. On the other hand, most of the boiling processes occur in nature also involve evolutions of multiple thermodynamic phases. That is, besides thermal convection, the fluid under goes a phase transition process in which liquid droplets and vapor bubbles are generated. The most obvious practical examples include the common water boiling in a pot.

We choose a standard Rayleigh-Benard setup, in which both the upper and the lower solid plates obey no-slip boundary conditions, while the horizontal boundary condition is periodic. To achieve more stable and second-order accurate numerical results, we have also applied the new scheme to the modified LB discretization formulation of He et al [11]. As discussed above, the Carnahan-Starling equation of state is used here for convenience. The mean density value $\rho = 1.36\rho_c$. The temperature on the upper wall is fixed at $T_u = 0.795T_c$ while on the lower wall $T_l = 0.954T_c$. Here T_c ($= 0.55$ in lattice units for the choice of the model) is the critical temperature for formation of two phases [11]. The initial temperature is set to be linearly distributed between the two plates and is consistent with their temperature boundary conditions. The simulation volume is $L \times H = 256 \times 128$ grid points. The gravity value $g = 5 \times 10^{-6}$ (lattice units) is used. In order to avoid unnecessary complications, a weak surface tension effect [8,11] is also applied in the LBM flow simulation, so that the surface tension contribution to the energy evolution can thus be neglected. Specifically, we choose the surface tension coefficient σ to be 0.01 for these simulations. The kinematic viscosity and the Prandtl number are set at $\nu = 0.02$ and $Pr = 10$, respectively. For simplicity, the heat capacity c_v in our multiphase flow is chosen as a constant ($= 1$). All the other fluid parameters are the same as in He et al [11]. Based on the choice of these parameter values, the resulting Rayleigh number is $Ra_a \sim 3.0 \times 10^5$, which is much higher than the first threshold ($Ra_c = 1708$) for an onset of convection in the conventional single-phase Rayleigh-Benard system [25].

The simulation starts from a uniform density distribution with one percent random

fluctuations. To enhance bubble formation, small temperature fluctuations are added to the equation of state in the first grid point layer near the bottom solid plate. Due to the higher temperature, a lower density fluid is produced that subsequently leads to small vapor bubbles at the bottom plate, and then these merge with each other to form larger size ones. The phase formation process in the simulation is combined with the convection process in which the hotter and lighter vapor phase rises while the colder and heavier liquid phase descends due to gravity. With the above choice of parameter values, such a full thermohydrodynamic cycle is seen to be able to sustain itself indefinitely. Figure 1 shows the density distributions at some representative nondimensionalized (by $\sqrt{H/g}$) times. One can observe the formation of two streams of bubbles near the bottom plate. One can also observe that two pairs of counter rotating convection rolls are locked between the bubble streams. In addition, the convection rolls are seen to pinch off the small bubbles from the bottom plate. As bubbles rise, their sizes are seen to increase slightly. Since small bubbles move faster than large bubbles, collision and coalescence often occur among them. Figure 2 shows streamlines of the velocity field at time 39.5, from which one can clearly see the two pairs of counter rotating convection rolls. Figure 3 depicts the corresponding temperature deviation from the linear distribution at the same time. Interestingly, the temperature exhibits a non-trivial behavior: Its value is seen to be relatively lower in the vapor phase domains near their interfaces. As expected physically, this phenomenon is due to the $p\nabla \cdot \mathbf{u}$ term in the energy equation (13) associated with the volume expansion from water to vapor phases. All the above simulated phenomena are qualitatively correct for a realistic two phase thermodynamic flow.

We also ran another simulation with the exact same setup as the above, except that the surface tension is made ten times stronger. As seen in figure 4, only one pair of counter rotating convection rolls is produced at its asymptotic state. Different from the standard single phase Bernard convection, we see that other intrinsic properties such as the surface tension can also alter the thermal convection characteristics in a multiphase flow [25].

IV. DISCUSSIONS

In this paper, we present a novel approach that combines a multiphase lattice Boltzmann method with a scalar temperature equation. The coupling is realized macroscopically via a self-consistent body-force. The basic formulation is applicable to both 2D and 3D flow situations. It is directly verifiable theoretically that new LB model obeys the correct full thermohydrodynamic equations with a non-ideal gas equation of state. The incorporation of thermohydrodynamics in the new approach allows for simulations of complex multiphase flows coupled with temperature dynamics. Other important features of the new scheme include its simplicity, efficiency and robustness for simulating thermal multiphase flow processes [26]. The latter has shown to be extremely difficult with the other LBM based schemes or the more conventional numerical methods [27]. Furthermore, like other LBMs, the new approach can handle complex physical boundary conditions [3]. All these are highly desirable for a practical computational model.

We have demonstrated the capability of our new approach for doing boiling flow simulations. This type of flows has so far not been successfully handled via other methods. Thus the new approach has opened a promising opportunity for numerically studying thermal multiphase flow problems. On the other hand, further improvements in the direction of the new approach are necessary in order for it to become a more useful and quantitative computational tool. Without going into detail, the major remaining issues include: 1) incorporating more realistic equations of state instead of the van der Waals type of gas model; 2) a more physical treatment of the heat capacity and latent heat; 3) further understanding and modeling of surface tension and near interface physics; 4) further enhancement of numerical stability to achieve significantly higher density ratio and lower viscosity; and 5) generalization of boundary conditions. Among all the above tasks, we consider (4) to be the most challenging one for LBM in general.

V. ACKNOWLEDGMENTS

The authors wish to thank Drs. Xiaoyi He, YueHong Qian, Ilya Staroselsky, Adrian Tenter, Steven Orszag, Sauro Succi, Rick Shock and Nick Martys for their useful discussions. This work is supported in part by DOE SBIR grant No. 65016B01-I.

REFERENCES

- [1] S. Chen and G. Doolen, *Ann. Rev. Fluid Mech.* **30**, 329 (1998).
- [2] U. Frisch, B. Hasslacher and Y. Pomeau, *Phys. Rev. Lett.* **56** (1986) 1505; and U. Frisch, D. d'Humières, B. Hasslacher, P. Lallemand, Y. Pomeau and J-P. Rivet, *Complex Systems* **1** (1987) 649.
- [3] H.D. Chen, C. Teixeira and K. Molvig, *Intl. J. Mod. Phys. C* **9**, No.8, 1281 (1998); C. Teixeira, *Intl. J. Mod. Phys. C* **9**, No.8, 1281 (1998); R. Lietz, S. Mallick, S. Kandasamy, H. Chen, *SAE*, No.2002-0154, (2002).
- [4] H.D. Chen, C. Teixeira and K. Molvig, *Int. J. Mod. Phys. C* **8**, 675 (1997).
- [5] S. Succi, H.D. Chen, C. Teixeira, G. Bella, A. De Maio, and K. Molvig, *J. Comp. Phys.*, **152**, 493 (1999); M. Pervaiz and C. Teixeira, *Proc. ASME PVP Conf.*, 2nd Intl. Sympo. on Comp. Techno. for Fluid/Thermal/Chem. Appl., Aug. 1-5, Boston, 1999.
- [6] S.-L. Hou, Ph.D. Thesis, Kansas State Univ., (1995).
- [7] D. Rothman, *Geophys.* **53**, 509 (1988); A. Gunstensen and D. Rothman, *J. Geophys. Res.* **98**, 6431 (1993); D. Grunau, S. Chen, and K. Eggert, *Phys. Fluids A* **5**, 2557 (1993).
- [8] R. Zhang, X. He and S.Y. Chen, *Comp. Phys. Comm.* **129**, 121 (2000).
- [9] Y. Qian, D. D'Humieres, and P. Lallemand, *Europhys. Lett.* **17**, 479 (1992); S.Y. Chen, H.D. Chen, D. Martinez, and W. Matthaeus, *Phys. Rev. Lett.* **67**, 3776 (1991); H.D. Chen, S.Y. Chen and W. Matthaeus, *Phys. Rev. A* **45**, 5339 (1992).
- [10] X. Shan and H.D. Chen, *Phys. Rev. E* **47**, 1815 (1993); X. Shan and H. Chen, *Phys. Rev. E* **49**, 2941 (1994).
- [11] X. He, S.Y. Chen and R. Zhang, *J. Comp. Phys.* **152**, 642 (1999); X. He, R. Zhang, S.Y. Chen and G.D. Doolen *Phys. of Fluids*, **11** 1143 (1999). X. He and G.D. Doolen, *J. Stat. Phys.* **107**, 309 (2002).

- [12] L. Reichl, “A modern course in statistical physics”, Univ. Texas Press, Austin, (1980).
- [13] G. R. McNamara and G. Zanetti, Phys. Rev. Lett. **61**, 2332 (1988).
- [14] Y. Qian, Ph.D. Thesis, Ecole Sup. Normale, Paris (1990).
- [15] R. Benzi, S. Succi, and M. Vergassola, Phys. Rep. **222**, 145 (1992).
- [16] X. Shan and X. He, Phys. Rev. Lett. **80**, 65 (1998); X. He and L. Luo, Phys. Rev. E **55**, 6333 (1997).
- [17] P. Bhatnagar, E. Gross, and M. Krook, Phys. Rev. **94**, 511 (1954).
- [18] N. Martys, X. Shan, and H. Chen, Phys. Rev. E **58**, 6855 (1998).
- [19] K. Huang, “Statistical Mechanics”, Wiley and Sons, 2nd Ed., New York (1987).
- [20] F. Alexander, S. Chen, and J. Sterling, Phys. Rev. E **47**, 2249 (1993); Y. Qian, J. Sci. Comp. **8**, No.3, 231 (1993).
- [21] C. Teixeira, H. Chen and D. Freed, Comp. Phys. Comm. **129**, 207 (2000).
- [22] A. Bartoloni, C. Battista, S. Cabasino, PS Paolucci, J. Peter, et al., Int. J. Mod. Phys. C **4**, 993 (1993); X. Shan, Phys. Rev. E **55**, 2780 (1997).
- [23] H.D. Chen, J. Stat. Phys. **81**, 347 (1995); H.D. Chen and C. Teixeira, Comp. Phys. Comm. **129**, 21 (2000).
- [24] Y. Qian and S. Chen, Intl. J. Mod. Phys. C **8**, 763 (1997).
- [25] S. Chandrasekhar, “Hydrodynamic and hydromagnetic stability”, Clarendon Press, Oxford (1961).
- [26] H.D. Chen, Computers in Physics **7**, No.6, 632 (1993).
- [27] R. Scardovelli and S. Zaleski, Ann. Rev. Fluid Mech. **31**, 567 (1999).

FIGURES

FIG. 1. Density distributions at $t = 39.5, 41.5, 43.5,$ and $45.5,$ respectively. Density ratio between liquid and vapor is 3. Red color represents the liquid phase, blue color represents the vapor phase.

FIG. 2. Streamline and vector plots of the flow velocity field at $t = 39.5.$

FIG. 3. Temperature deviation ($T_{dev} = \frac{T - T_{linear}}{T_{top}}$) at $t = 39.5.$ The color range is $(-0.1, 0.02).$

FIG. 4. Density distribution and velocity vector plot with surface tension coefficient $\sigma = 0.1.$

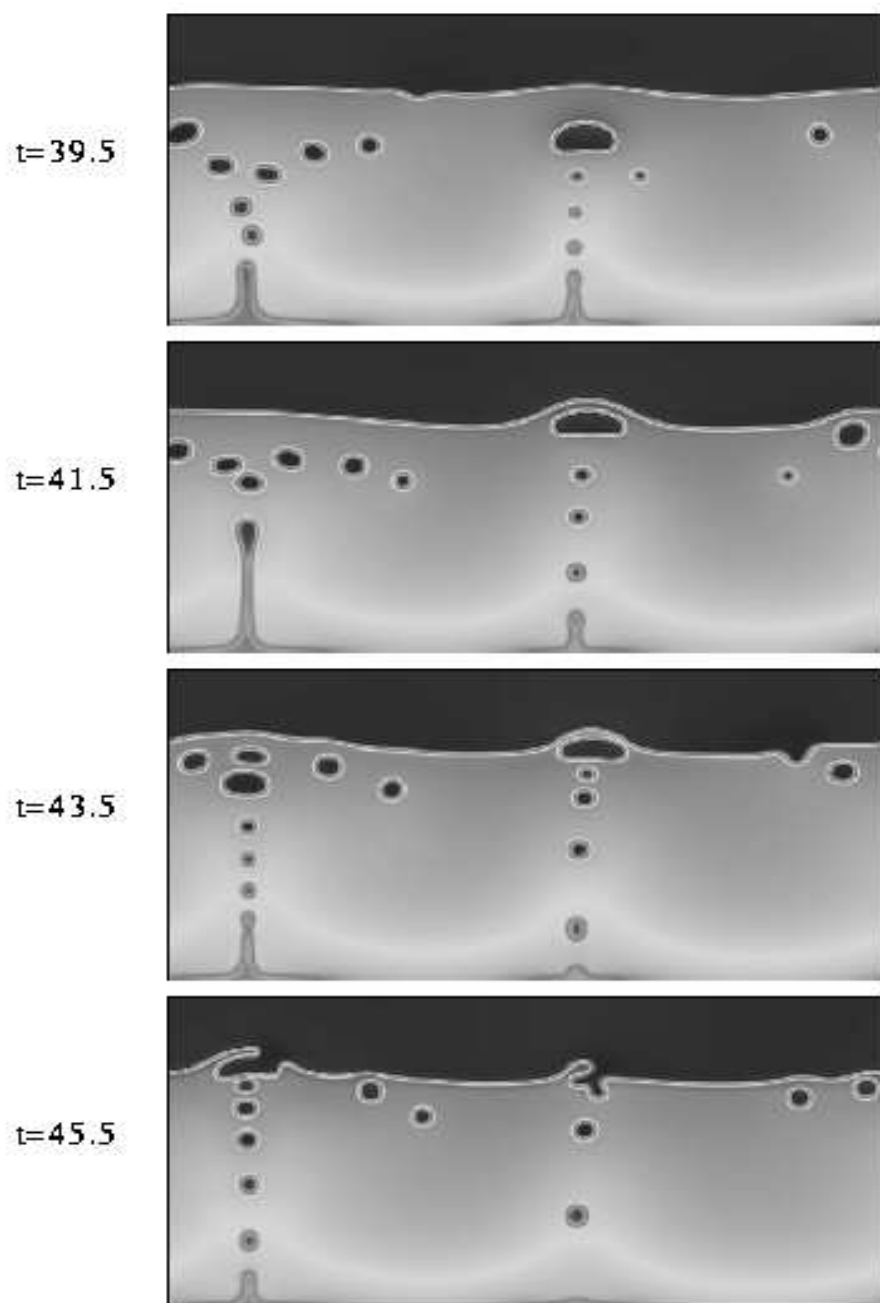


FIG. 1.

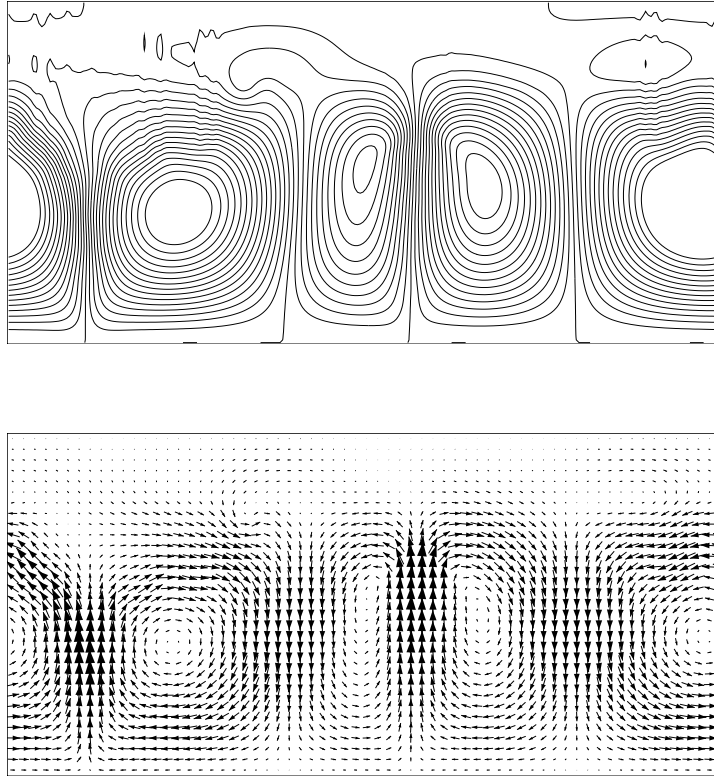


FIG. 2.

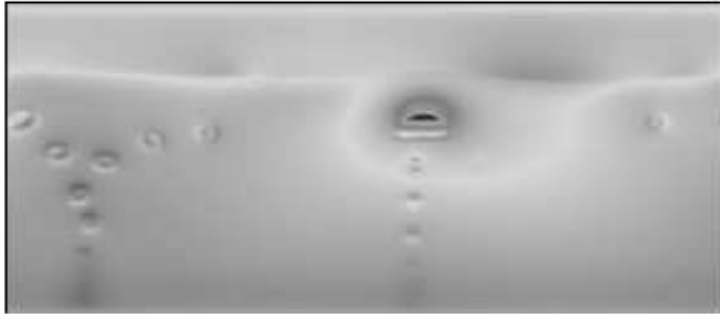


FIG. 3.

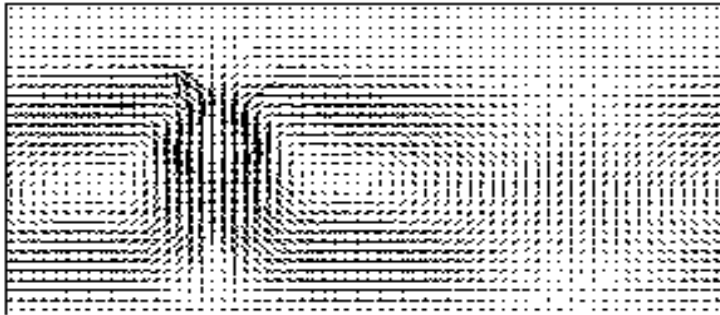
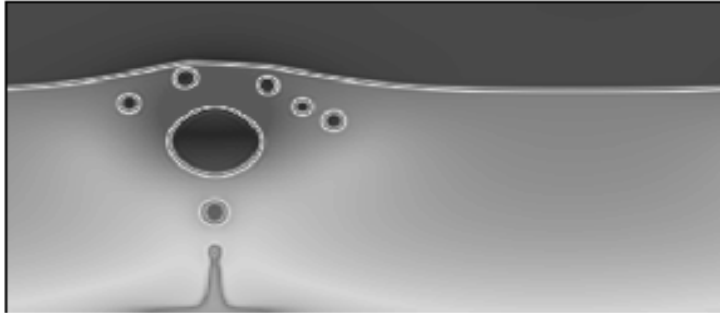


FIG. 4.